JOURNAL OF PHARMA INSIGHTS AND RESEARCH ISSN NO. 3048-5428

RESEARCH ARTICLE

Development of Functionalized 1,2,4-Triazole Derivatives as Potential Aromatase Inhibitors in Breast Cancer

Eligros Kujur, Laxmi Banjare*

Department of Pharmaceutical Chemistry, Shri Shankaracharya Professional University, Bhilai, Chhattisgarh, India

Publication history: Received on 19th January 2026; Revised on 27th February 2026; Accepted on 28th February 2026

Article DOI: 10.69613/hmd42z94

Abstract: Breast cancer is characterized by high morbidity and mortality rates largely driven by estrogen-dependent tumor proliferation. The enzyme aromatase, a member of the cytochrome P450 superfamily, catalyzes the rate-limiting step in estrogen production, rendering it a critical focal point for therapeutic intervention. Although existing clinical inhibitors offer efficacy, their long-term administration is frequently compromised by systemic toxicity and the acquisition of drug resistance. This research details the rational design and microwave-accelerated preparation of a novel series of 1,2,4-triazole analogues (4a-f). Structural elucidation of the resulting derivatives was achieved through rigorous spectroscopic analysis, including FTIR, NMR, and Mass spectrometry. The pharmacological potential was characterized via DPPH radical scavenging and MTT cytotoxicity assays against the MCF-7 human breast adenocarcinoma cell line. Computational insights were garnered through molecular docking simulations utilizing human placental aromatase (PDB ID: 3S79) to map the binding orientation and energetic stability. Experimental data identified compound 4c as the most potent candidate, exhibiting an IC50 of 24.78 ± 0.87 μM in antioxidant assays and superior growth inhibition in MCF-7 cells. Structure-activity relationship assessments indicate that electron-donating functionalities on the aromatic ring significantly enhance biological potency. Molecular docking correlated with these findings, as compound 4c demonstrated a MolDock score of -151.841 kcal/mol, indicating a higher binding affinity than the reference drug Letrozole. These observations position the triazole-based scaffold as a viable lead for the progression of next-generation aromatase inhibitors in oncology.

Keywords: 1,2,4-Triazole analogues; Aromatase inhibitors; Breast adenocarcinoma; Molecular docking; Cytotoxicity.

1. Introduction

Breast cancer is the most prevalent malignancy among the female population, representing a substantial portion of the global oncology burden and the leading cause of cancer-associated mortality [1]. Statistics from recent epidemiological studies indicate that the incidence of this disease continues to rise, with millions of new cases diagnosed annually, necessitating more robust therapeutic strategies to combat tumor progression and recurrence [2]. Despite improvements in early detection and multimodal treatment regimens, the clinical management of advanced stages remains difficult due to the emergence of refractory phenotypes and the off-target effects associated with conventional chemotherapy [3].

A significant proportion of breast tumors are hormone-responsive, relying on localized estrogen production for cellular proliferation and survival. The enzyme aromatase (CYP19A1) is the solitary enzyme in the human body capable of converting androgens specifically androstenedione and testosterone into estrogens via an oxidative aromatization process [4]. Consequently, the inhibition of aromatase has surfaced as a cornerstone in the treatment of postmenopausal women with hormone-receptor-positive breast cancer [5]. While third-generation inhibitors such as Letrozole and Anastrozole have revolutionized clinical outcomes, their prolonged use is often associated with musculoskeletal issues and bone density loss, highlighting the demand for molecules with improved selectivity and safety profiles [5].

Heterocyclic chemistry provides a vast library of "privileged scaffolds," among which the 1,2,4-triazole nucleus is particularly notable for its metabolic stability and diverse biological profile [6]. The triazole ring possesses a high dipole moment and the ability to act as both a hydrogen bond donor and acceptor, which facilitates strong interactions with biological macromolecules. In the context of aromatase inhibition, the nitrogen atoms within the triazole ring are uniquely positioned to coordinate with the heme iron at the enzyme's active site, effectively blocking the catalytic cycle. This specific interaction mechanism makes triazole derivatives highly promising for the development of potent and targeted anticancer agents [7].

* Corresponding author: Laxmi Banjare

The current research focused on the molecular derivation of a series of novel triazole-linked analogues designed to occupy the catalytic pocket of the aromatase enzyme more effectively. This work aimed to optimize the electronic density and hydrophobic interactions required for peak inhibition by incorporating various substituents on the phenylhydrazine and benzohydrazide moieties. The work integrates chemical construction via microwave-assisted protocols, comprehensive spectroscopic characterization, biological screening, and computational modeling to validate the potential of these derivatives as future therapeutic candidates.

2. Materials and Methods

2.1. Chemicals and Instruments

The chemical reagents and solvents utilized in this study were of analytical grade, sourced from reputable suppliers including Sigma-Aldrich, Merck, and Loba Chemie. Reaction monitoring was performed via Thin-Layer Chromatography (TLC) using silica gel G plates. Melting points were determined using an open capillary method. Spectroscopic data were acquired using a Bruker Advance Neo 400 MHz NMR spectrometer (DMSO-d6) and a PerkinElmer Spectrum IR. Mass spectra were generated on an Xevo G2-XS QT quadrupole time-of-flight mass spectrometer.

2.2. Chemistry of Triazole Derivatives

2.2.1 Procedure for the synthesis of 1H-1,2,4-triazol-3-amine (1)

Aminoguanidine (0.01 mol) and formic acid (0.01 mol) were dissolved in ethanol (10 mL) in the presence of KOH and subjected to microwave irradiation (280 W, 60-65 °C) in two runs for 10 minutes. After completion, the reaction mixture was cooled, neutralized with dilute HCl, and acetone was added to induce precipitation. The resulting solid was filtered, washed with cold acetone, and dried to obtain the desired compound.

IR (KBr, cm^{-1}): 3352.44 (N-H), 3297.74 (N-H), 1645.68 (C=N), 1550.44 (N-N), 1267.35 (C-N); ^{1}H NMR (400 MHz, DMSO-d_6) δppm: 5.57-5.87, 7.79-8.07, 10.87-11.32; ^{13}C NMR (400 MHz, DMSO-d_6) δppm: 147.80, 152.44.

2.2.2 Procedure for the synthesis of 4-(((1H-1,2,4-triazol-3-yl) imino) methyl) benzonitrile (2)

Compound 1 (0.01 mol) and cyanobenzaldehyde (0.01 mol) were dissolved in ethanol with a catalytic amount of acetic acid and subjected to microwave irradiation (280 W, 50-60 °C) for 15 minutes. After completion, crushed ice was added, and the mixture was left to stand for 30 minutes to allow precipitation. The solid product was then filtered, washed with cold water or ethanol, and dried to obtain the desired compound.

IR (KBr, cm^{-1}): 3045.74 (Ar C-H), 2232.69 (C≡N), 1644.82 (C=N), 1586.41 (C=C), 1548.59 (N-N), 1234.62 (C-N); ^{1}H NMR (400 MHz, DMSO-d_6) δppm: 7.21-7.32, 7.43-7.61, 7.71-7.92, 8.20-8.42, 8.53-8.74, 11.07-11.40; ^{13}C NMR (400 MHz, DMSO-d_6) δppm: 112.82, 118.35, 121.41, 126.16, 128.62, 130.50, 136.71, 145.84, 149.61, 152.33.

2.2.3 Procedure for the synthesis of 4-(((1-(3-oxobutyl)-1H-1,2,4-triazol-3-yl) imino) methyl) benzonitrile (3)

The compound (0.01 mol) was dissolved in acetone with formaldehyde, and 10% KOH was added as a base catalyst. The mixture was subjected to microwave irradiation (280 W, 50-60 °C) for 20 minutes. After cooling, it was neutralized with dilute HCl and poured onto crushed ice to precipitate the product. The solid was filtered, washed with cold water, and dried to obtain the desired compound.

IR (KBr, cm^{-1}): 3064.72 (Ar C-H), 2862.19 (Alp C-H), 2228.34 (C≡N), 1664.80 (C=O), 1671.45 (C=C), 1560.61 (C=N), 1259.26 (C-N); ^{1}H NMR (400 MHz, DMSO-d_6) δppm: 2.04-2.15, 2.60-2.79, 3.18-3.40, 7.52-7.71, 7.77-7.95, 8.18-8.40, 8.51-8.71; ^{13}C NMR (400 MHz, DMSO-d_6) δppm: 29.85, 34.70, 41.55, 112.92, 118.46, 121.33, 126.42, 128.91, 131.03, 145.70, 149.35, 152.24, 197.60.

2.2.4 Procedure for the synthesis of N'-(4-(3-((substitutedbenzylidene) amino)-1H-1,2,4-triazol-1-yl) butan-2-ylidene) isonicotinohydrazide (4a-f)

Compound 3 (0.01 mol) and the appropriate hydrazide derivative (0.01 mol) were dissolved in ethanol as a solvent in the presence of a catalytic amount of glacial acetic acid. The reaction mixture was transferred to a microwave-compatible vessel and irradiated at 350 W (60-70 °C) for 15-20 minutes. After completion, the mixture was cooled to room temperature, neutralized with dilute HCl, and poured onto crushed ice to induce precipitation. The resulting solid was filtered, washed with cold water or ethanol, and dried to obtain the desired compound.

a. N'-(4-(3-((4-cyanobenzylidene) amino)-1H-1,2,4-triazol-1-yl) butan-2-ylidene) isonicotinohydrazide (4a):

Color: yellow powder; % Yield: 82.45; M.P.: 81-83 °C; IR (KBr, cm^{-1}): 3365.41 (N-H), 3062.74 (Ar C-H), 2925 (Alp C-H), 2226.45 (C≡N), 1665.74 (C=O), 1618.40 (C=N), 1565.74 (Ar C=C); ^{1}H NMR (400 MHz, DMSO-d_6) δppm: 2.11, 2.61, 4.02, 7.54, 7.81, 7.98, 8.77. 9.53, 10.86; ^{13}C NMR (400 MHz, DMSO-d_6) δppm: 19.8, 29.5, 42.1,114.8, 118.4, 121.7, 126.1, 132.2, 140.6, 143.7, 149.4, 158.1, 163.1; MS: calculated [M^+] m/z Found: 386.12; Elemental Analysis Found: C, 62.11; H, 4.68; N, 28.98; O, 4.11.

b. 4-(((1-(3-(2-phenylhydrazineylidene) butyl)-1H-1,2,4-triazol-3-yl)imino)methyl) benzonitrile (4b):

Color: off white powder; % Yield: 83.54; M.P.: 80-84 °C; IR (KBr, cm^{-1}): 3365.85 (N-H), 3072.85 (Ar C-H), 2942.74 (Alp. C-H), 2234.52 (C≡N), 1618.72 (C=N), 1561.25 (Ar C=C); ^{1}H NMR (400 MHz, DMSO-d_6) δppm: 1.93, 2.60, 4.01, 7.05, 7.32, 7.53, 7.98, 8.76 8.97; ^{13}C NMR (400 MHz, DMSO-d_6) δppm: 14.1, 23.7, 42.0, 113.9, 114.6, 118.6, 122.3, 126.2, 132.2, 140.5, 143.7, 158.1, 158.4; MS: calculated [M^+] m/z Found: 357.05; Elemental Analysis Found: C, 67.15; H, 5.22; N, 27.34.

c. N'-(4-(3-((4-cyanobenzylidene) amino)-1H-1,2,4-triazol-1-yl) butan-2-ylidene)-4-methylbenzohydrazide (4c)

Color: white powder; % Yield: 79.85; M.P.: 85-88 °C; IR (KBr, cm^{-1}): 3365.81 (N-H), 3069.75 (Ar C-H), 2922.75 (Alp. C-H), 2221.45 (C≡N), 1661.70 (C=O), 1618.45 (C=N), 1526.74 (Ar C=C); ^{1}H NMR (400 MHz, DMSO-d_6) δppm: 1.92, 2.40, 2.60. 4.01, 7.30, 7.52, 7.82, 7.98, 9.52, 10.82; ^{13}C NMR (400 MHz, DMSO-d_6) δppm: 10.0, 13.7, 31.4, 42.4, 114.4, 118.1, 126.2, 140.6, 143.6, 158.2, 160.4; MS: calculated [M^+] m/z Found: 399.11; Elemental Analysis Found: C, 66.10; H, 5.22; N, 24.51; O, 4.00.

d. N'-(4-(3-((4-cyanobenzylidene) amino)-1H-1,2,4-triazol-1-yl) butan-2-ylidene) propionohydrazide (4d)

Color: white powder; % Yield: 76.15; M.P.: 80-83 °C; IR (KBr, cm^{-1}): 3361.78 (N-H), 3061.85 (Ar C-H), 2929.54 (Alp. C-H), 2232.15 (C≡N), 1653.16 (C=O), 1617.19 (C=N), 1532.74 (Ar C=C); ^{1}H NMR (400 MHz, DMSO-d_6) δppm: 1.01, 1.90, 2.26, 2.60, 7.53, 7.94, 8.73, 9.54, 10.53; ^{13}C NMR (400 MHz, DMSO-d_6) δppm: 10.2, 13.4, 31.5, 42.0, 114.5, 118.2, 126.2, 140.5, 143.7, 158.0, 160.2; MS: calculated [M^+] m/z Found: 337.17; Elemental Analysis Found: C, 60.44; H, 5.58; N, 29.01; O, 4.62.

e. 4-amino-N'-(4-(3-((4-cyanobenzylidene) amino)-1H-1,2,4-triazol-1-yl) butan-2-ylidene) benzohydrazide (4e)

Color: white powder; % Yield: 76.82; M.P.: 82-86 °C; IR (KBr, cm^{-1}): 3362.41 (N-H), 3452.45 (-NH_2), 3062.75 (Ar C-H), 2921.50 (Alp. C-H), 2224.40 (C≡N), 1661.07 (C=O), 1634.41 (C=N), 1567.15 (Ar C=C); ^{1}H NMR (400 MHz, DMSO-d_6) δppm: 1.90, 2.60, 4.01, 5.44, 6.50, 7.52, 7.53, 9.54, 10.44; ^{13}C NMR (400 MHz, DMSO-d_6) δppm: 13.7, 42.0, 114.2, 118.6, 122.3, 126.7, 132.1, 151.3, 158.2, 160.4; MS: calculated [M^+] m/z Found: 400.11; Elemental Analysis Found: C, 62.85; H, 5.01; N, 27.72; O, 3.85.

f. N'-(4-(3-((4-cyanobenzylidene) amino)-1H-1,2,4-triazol-1-yl) butan-2-ylidene) formohydrazide (4f)

Color: white powder; % Yield: 80.75; M.P.: 84-86 °C; IR (KBr, cm^{-1}): 3349.75 (N-H), 3063.04 (Ar C-H), 2925.74 (Alp. C-H), 2224.40 (C≡N), 1682.85 (C=O), 1620.74 (C=N), 1581.72 (Ar C=C); ^{1}H NMR (400 MHz, DMSO-d_6) δppm: 1.91, 2.60, 7.52, 7.97, 8.19, 8.76, 9.52, 10.84; ^{13}C NMR (400 MHz, DMSO-d_6) δppm: 13.5, 23.5, 42.01, 117.5, 125.6, 132.1, 143.6, 158.1, 166.0; MS: calculated [M^+] m/z Found: 309.12; Elemental Analysis Found: C, 58.20; H, 4.73; N, 31.65; O, 5.12

2.3. Pharmacological Activities

2.3.1. Antioxidant activity

The DPPH (2, 2-diphenyl- 1-picrylhydrazyl) free radical scavenging test assessed the ability of the synthesized compounds (4a-f) to act as antioxidants. Each compound was made up (10 mM into stock solutions in ethanol and then diluted to form a concentration range of 5-25 μM/mL. In the case of assay, 0.1 mL of each test solution was mixed with 3 mL of a 0.1 mM solution of DPPH. The mixtures of the reaction were kept in the dark at room temperature to allow a full interaction between the antioxidant compounds and DPPH radicals. A UV-Visible spectrophotometer was used to measure the decrease in absorbance at 517 nm. A control was made using the DPPH solution in place of the test sample using DMSO. The radical scavenging activity was determined by associating the absorbance of the test samples with that of the control [8].

2.3.2. Cytotoxicity study

The MTT assay of the cytotoxic activity of the compounds (4a-f) was done on MCF-7 human cancer cell lines. Cells were seeded at a cell density of 2.5 thinly sliced cells/well (or 2.5 lives/plate) in 96-well plates, incubated at 370 C in a moist 5% CO2 environment to allow the cells to bond. Washing in PBS was done, followed by treatment of cells with various concentrations of the compounds

(200 nM, 2, 5, 10, and 20 nM) and 72h of incubation. Then 10 µL of MTT solution was put in each well and incubated for 4 h in order to allow the formation of formazan crystals. They dissolved the crystals with 10% SDS in 0.01 N HCl, and the absorbance was measured at 562 nm by a microplate reader, and cell viability was determined against an untreated control [9].

2.4. 4. Molecular Docking

Molecular docking analyses were conducted to understand the binding affinities and binding profiles of the prepared triazole analogs (4a-f) with human placenta aromatase cytochrome P450. Two-dimensional (2D) chemical representations of all target compounds, as well as a reference inhibitor, Letrozole, were generated in ChemDraw 22.2.0. Energy minimization of these structures was then done with the help of the MM2 force field to get the most thermodynamically stable conformational structures. The optimized geometries were then transformed to three-dimensional (3D) format and stored as 3D PDB files to be used in subsequent computational analysis [10]. Human placental aromatase is a crystallographic structure that was obtained at The RCSB Protein Data Bank (PDB ID: 3S79; resolution: 2.75 A) [11]. Protein preparation consisted of all crystallographic water molecules and co-crystallized ligands removed, and necessary hydrogen atoms added to stabilize the structure to use in docking simulations. Molegro Virtual Docker v6.0 was used to carry out molecular docking simulations, which included an advanced cavity detection algorithm that was used to identify potential ligand-binding sites. The grid box dimension was set at 30 X30 X30 A, centred around the active site region, being X: -0.92, Y: 52.67, and Z: 6.75 with a radius of 15.0 A about the active site region. Docking resolution was set to 0.30 A, to provide accuracy in the positioning of the ligand. To promote the reliability and strength of the docking results, every ligand was docked 10 times in separate docking replicates, using a population size of 50 and a maximum of 1500 docking iterations per replicate, thus allowing exhaustive conformational sampling. The highest docking poses were chosen using binding energy values and stability of the interactions [12]. Lastly, the binding orientations, intermolecular interactions, and amino acid residues of the active site that bind to the ligand were carefully analyzed and visualized with BIOVIA Discovery Studio Visualizer [13].

3. Results and Discussion

3.1. Chemistry

The synthesized compounds (4a-f) were successfully confirmed by spectral data, showing the formation of the targeted triazole-based derivatives. Compound (1) exhibited characteristic IR peaks at 3352.44 and 3297.74 cm^{-1} (N-H), 1645.68 cm^{-1} (C=N), 1550.44 cm^{-1} (N-N), and 1267.35 cm^{-1} (C-N), while ^{1}H NMR signals at δ 5.57-5.87, 7.79-8.07, and 10.87-11.32 ppm supported the presence of NH and heteroaromatic protons, further confirmed by ^{13}C NMR signals at δ 147.80 and 152.44 ppm.

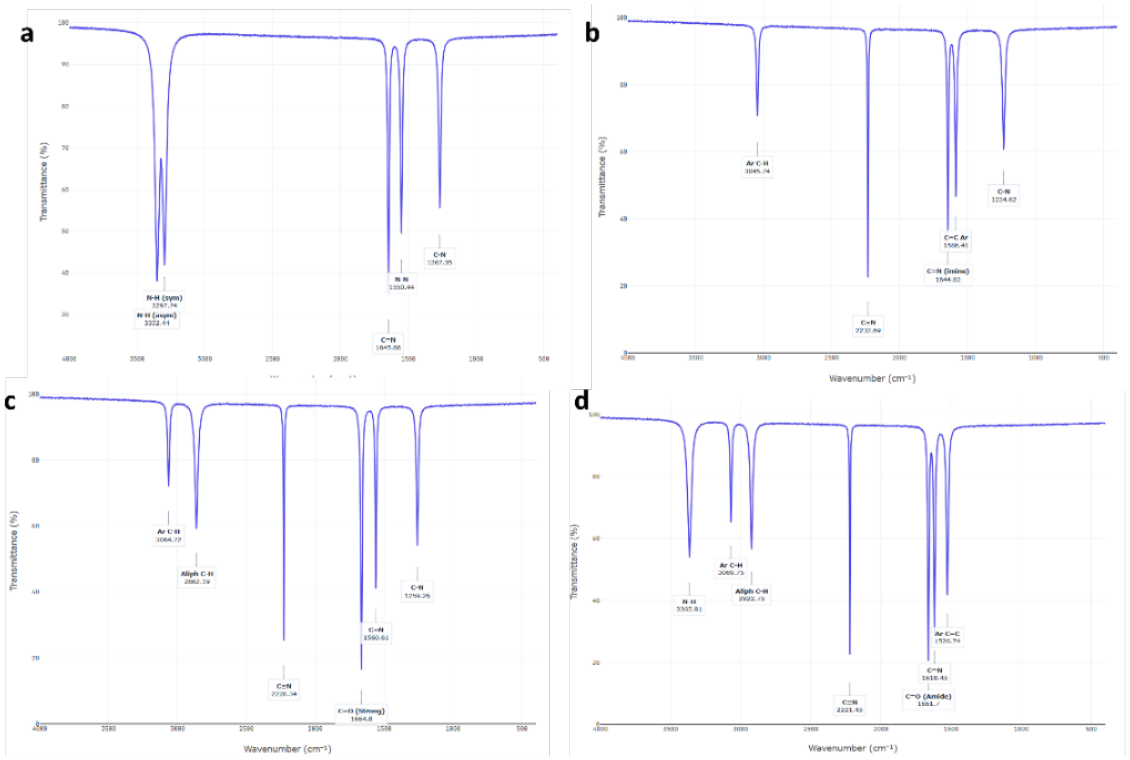

Figure 1. FTIR spectrum of a. Amine Scaffold b. Nitrile Intermediate c. Butanone Intermediate and d. Active Lead

Compound (2) showed absorption bands at 3045.74 cm^{-1} (Ar C-H), 2232.69 cm^{-1} (C≡N), 1644.82 cm^{-1} (C=N), and 1586.41 cm^{-1} (C=C), with ^1H NMR signals in the aromatic region δ 7.21–8.74 ppm and NH at δ 11.07-11.40 ppm, while ^{13}C NMR signals (δ 112.82-152.33 ppm) confirmed aromatic and nitrile carbons. Compound (3) displayed peaks at 3064.72 cm^{-1} (Ar C–H), 2862.19 cm^{-1} (aliphatic C-H), 2228.34 cm^{-1} (C≡N), 1664.80 cm^{-1} (C=O), and 1560.61 cm^{-1} (C=N), with ^1H NMR signals at δ 2.04-3.40 ppm (aliphatic) and δ 7.52-8.71 ppm (aromatic), and a characteristic carbonyl carbon at δ 197.60 ppm in ^{13}C NMR. The final derivatives (4a-f) consistently exhibited IR bands in the range 3349.75-3365.85 cm^{-1} (N-H), 3061.85-3072.85 cm^{-1} (Ar C-H), 2921.50-2942.74 cm^{-1} (aliphatic C-H), 2221.45-2234.52 cm^{-1} (C≡N), 1653.16-1682.85 cm^{-1} (C=O), 1617.19-1634.41 cm^{-1} (C=N), and 1526.74-1581.72 cm^{-1} (Ar C=C), confirming the presence of key functional groups. The ^1H NMR spectra revealed signals for aliphatic protons (δ 1.01-4.02 ppm), aromatic protons (δ 7.05-8.77 ppm), and -NH protons (δ 9.52-10.86 ppm), while ^{13}C NMR data (δ 10.0-166.0 ppm) further supported the structural framework. Mass spectra showed molecular ion peaks consistent with calculated values (m/z 309.12-400.11), and elemental analysis data were in close agreement with theoretical compositions, confirming the effective synthesis and purity of the compounds.

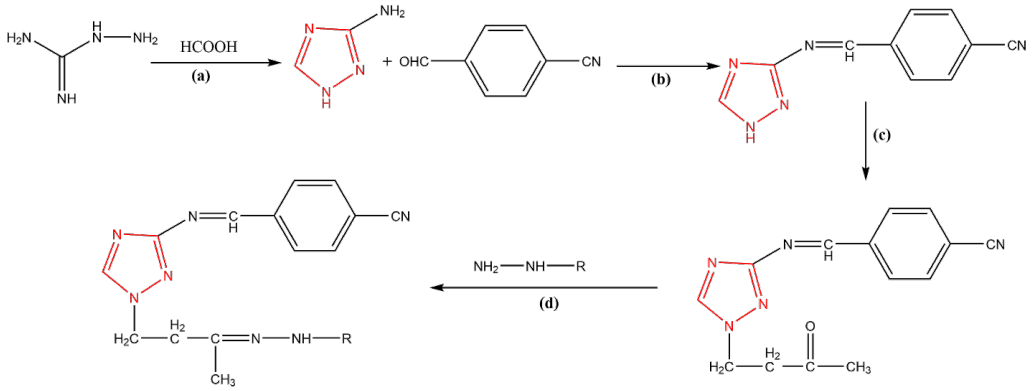

Scheme 1. Synthetic strategies of novel 1,2,4-triazole derivatives (4a-f).

Reaction Conditions: KOH, ethanol, 280 W, 60-65 °C, reflux, 10 minutes, (b) Ethanol, acetic acid, 280 W, 50-60 °C, reflux, 15 minutes, (c) 10% KOH, microwave irradiation 280 W, 50-60 °C, reflux, 20 minutes, (d) glacial acetic acid, 350 W, 60-70 °C, reflux, 15-20 minutes.

Table 1. Structures of the compounds 4a to 4f

Compound ID	Structure
4a	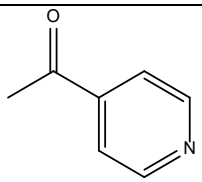
4b	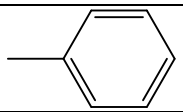
4c	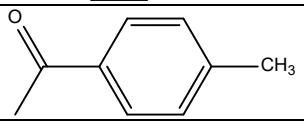
4d	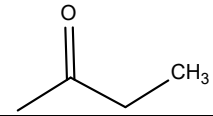
4e	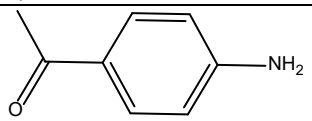
4f	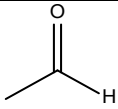

3.2. Pharmacological Activities

3.2.1. Antioxidant activity

The antioxidant activity of the synthesized 1,2,4-triazole derivatives (4a-f) was assessed using the DPPH free radical scavenging assay, with Ascorbic acid as the standard (Table 2). The IC_{50} values indicated that compounds 4c (24.78 ± 0.87 μM) and 4b (28.51 ± 0.52 μM) exhibited superior antioxidant activity compared to the reference drug (32.05 ± 1.29 μM), followed by 4a (30.47 ± 0.61 μM), while compounds 4d (48.44 ± 1.54 μM), 4e (54.03 ± 2.11 μM), and 4f (57.73 ± 2.07 μM) exhibited comparatively lower activity (Figure 2). Structure-activity relationship (SAR) analysis revealed that the enhanced activity of compounds 4c, 4b, and 4a can be attributed to the presence of electron-donating substituents, which increase electron density on the aromatic system and facilitate effective hydrogen or electron donation to stabilize the DPPH radical via resonance. In contrast, derivatives bearing electron-withdrawing groups (4a-f) showed reduced radical scavenging potential due to reduced electron density, limiting their ability to neutralize free radicals. These results highlight the crucial role of electronic effects in modulating the antioxidant efficiency of the triazole scaffold.

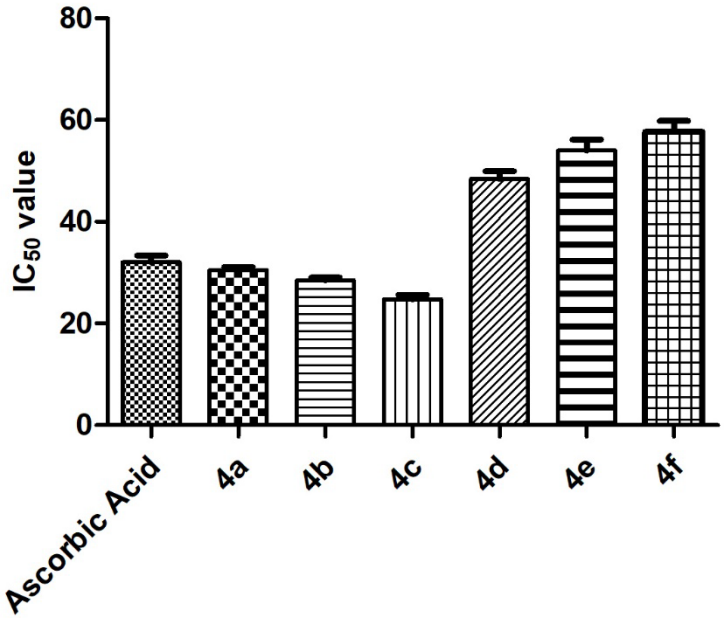

Figure 2. Antioxidant activity of 1,2,4-triazole derivatives (4a-f).

Table 2. Antioxidant activity of 1,2,4-triazole derivatives (4a-f).

Compound ID	IC_{50} Value[a]
Ascorbic acid	32.05 ± 1.29
4a	30.47 ± 0.61
4b	28.51 ± 0.52
4c	24.78 ± 0.87
4d	48.44 ± 1.54
4e	54.03 ± 2.11
4f	57.73 ± 2.07

[a] IC_{50} Value expressed in μM±SEM.

3.2.2. Cytotoxicity Study

The cytotoxic activity of the synthesized 1,2,4-triazole derivatives (4a–f) against the MCF-7 breast cancer cell line revealed a clear structure-activity relationship (SAR) influenced by the nature of substituents on the aromatic ring. Among all derivatives, compound 4c exhibited the highest anticancer activity, showing a marked reduction in cell viability even at 200 nM, which may be attributed to the presence of a methyl-substituted aromatic ring (electron-donating group) that enhances electron density, thereby improving interaction with intracellular targets and promoting apoptotic pathways. Compound 4b, bearing a phenyl group, also established significant cytotoxicity with activity comparable to the standard drug Letrozole, suggesting favorable hydrophobic and π-π

interactions with biological macromolecules. Compound 4a showed moderate activity, likely due to the presence of a heteroaromatic moiety, which contributes to balanced electronic and steric effects. In contrast, compounds 4d and 4f, containing aliphatic substituents (propionyl and formyl groups), exhibited reduced cytotoxicity, indicating that the absence of aromatic conjugation diminishes binding affinity and cellular uptake (Figure 3). Compound 4e, despite having an -NH_2 group (electron-donating), showed comparatively lower activity, possibly due to increased polarity affecting membrane permeability. Overall, the results suggest that electron-donating and aromatic substituents significantly increase anticancer activity, while aliphatic or highly polar groups reduce efficacy. These results indicate compound 4c as the most promising candidate, with 4b also can serve as a potential lead for further optimization in anticancer drug development.

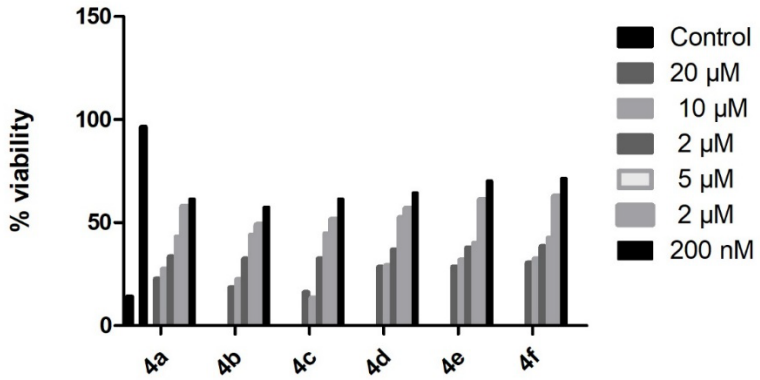

Figure 3. Cytotoxicity study of 1,2,4-triazole derivatives (4a-f).

3.3. Molecular Docking

Molecular docking studies using Molegro Virtual Docker version 6.0 revealed that the synthesized 1,2,4-triazole derivatives (4a-f) displayed strong binding affinity toward Human placental aromatase (PDB ID: 3S79), a key enzyme involved in estrogen biosynthesis and breast cancer progression. The docking results (Table 3) exhibited MolDock scores ranging from -121.952 to -151.841 kcal/mol, with compound 4c displaying the highest binding affinity (-151.841 kcal/mol), surpassing the reference drug Letrozole (-132.837 kcal/mol). The enhanced binding is attributed to stabilizing interactions such as hydrogen bonding, π-π stacking, and sulfur interactions with crucial amino acid residues. Notably, compound 4c formed multiple hydrogen bonds with Trp141, Ser314, Cys437, and Gly439, along with hydrophobic interactions involving Ile132 and Arg435, conducive to complex stability. Also, compound 4b displayed interaction patterns comparable to Letrozole, particularly with Ser478 and Glu483, as shown in Figure 3. Significantly, residues such as Ser314, Cys437, Trp141, and Glu483 are essential for aromatase activity, and their inhibition may suppress estrogen production, a key strategy in hormone-dependent breast cancer treatment. Molecular visualization of the protein-ligand complex of compound 4b and the standard drug is shown in Figure 4 indicate that the synthesized compounds possess promising potential as aromatase inhibitors, warranting further biological evaluation.

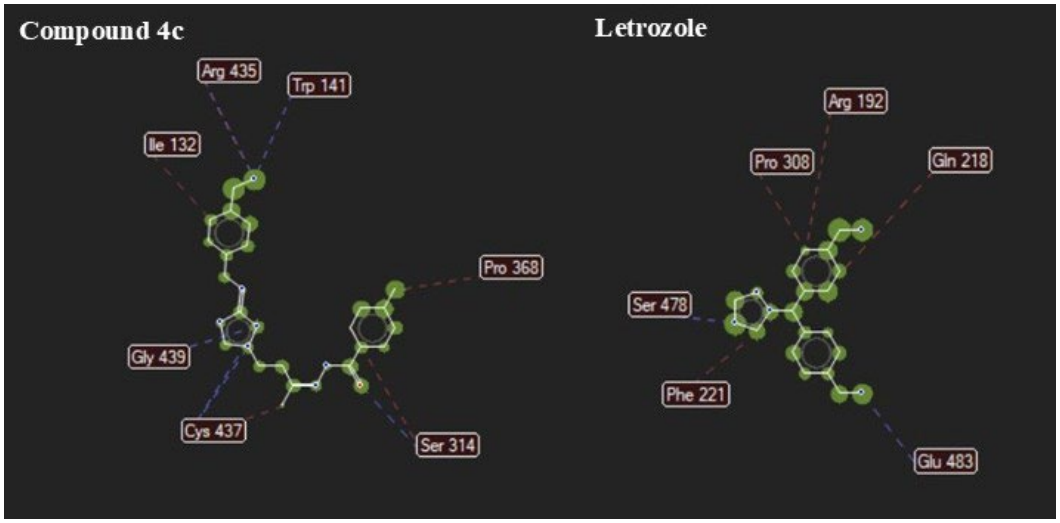

Figure 3. Comparative binding interactions of compound 4c and the reference drug Letrozole within the active site of the target protein.

Table 3. Molecular docking simulations of designed 1,2,4-triazole derivatives.

Compound ID	MolDock Score (kcal/mol)	Interaction (kcal/mol)	H-Bond (kcal/mol)	H-bonds Interaction	S-bonds Interaction
Letrozole	-132.837	-161.029	-4.86701	Ser478, Glu483	Arg192, Gln218, Phe221, Pro308
4a	-146.743	-119.474	-6.26471	Trp141, Ser314, Cys437, Ala438, Arg435,	lle132, Cys437,
4b	-149.465	-85.9401	-6.08579	Ser314, His402, Cys310, Glu483	Gln218, Ser314,
4c	-151.841	-122.876	-7.55549	Trp141, Ser314, Cys437, Gly439	lle132, Trp141, Ser314, Arg435
4d	-121.952	-110.348	-5.37839	Ser314, Cys437, Gly439	Phe317, Ser363, Val369
4e	-129.063	-32.2228	-4.45422	Ser314, His402 Cys437, Gln367	Pro368, lle398, Ser363, Val369
4f	-136.413	-73.5388	-7.81719	Ser314, His402	Thr310, Ser314, Pro368, lle398, Ser363, Val369

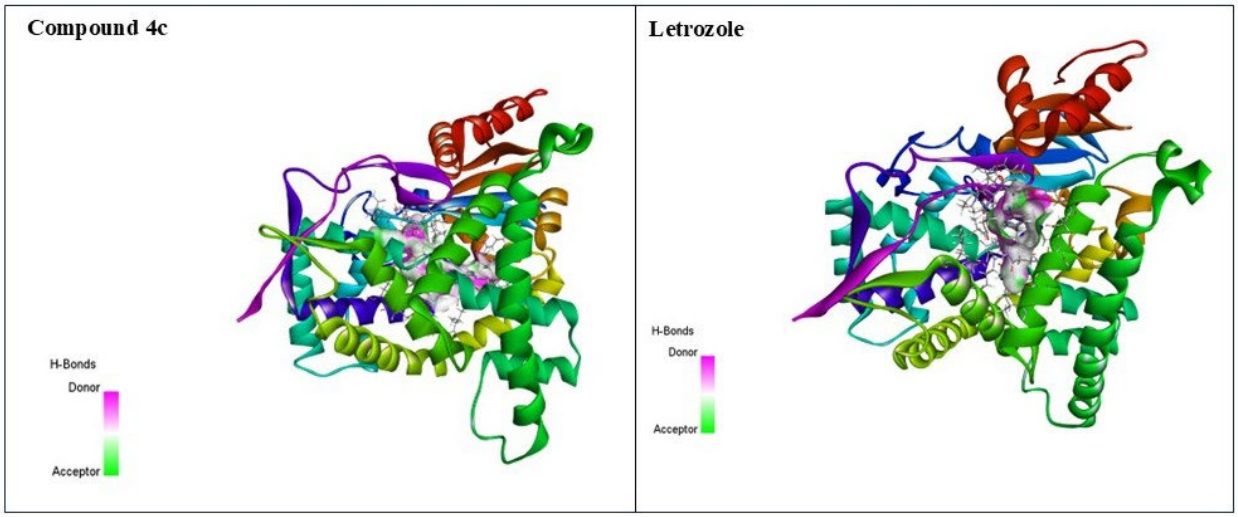

Figure 5. Three-dimensional visualization of the docked poses of compound 4c and the reference drug Letrozole within the active site of the target protein.

4. Conclusion

This research work had shown the successful preparation and biological evaluation of a novel series of 1,2,4-triazole-based derivatives as potential therapeutic agents for breast cancer. Synthesis was efficiently achieved through microwave-assisted methods, providing high yields and high purity. Biological assays proved that compound 4c possesses superior antioxidant and cytotoxic properties, with its performance exceeding that of the standard reference drugs in several parameters. Molecular docking analysis provided a structural basis for these results, confirming that the triazole-linked analogues fit precisely within the aromatase catalytic site, forming stable complexes via hydrogen bonding and hydrophobic contacts. The results indicate compound 4c as a highly promising lead candidate for the development of targeted aromatase inhibitors.

References

[1] Sung H, Ferlay J, Siegel RL, Laversanne M, Soerjomataram I, Jemal A, et al. Global Cancer Statistics 2020: GLOBOCAN Estimates of Incidence and Mortality Worldwide for 36 Cancers in 185 Countries. CA Cancer J Clin. 2021;71(3):209-49.

[2] Ferlay J, Ervik M, Lam F, Colombet M, Mery L, Piñeros M, et al. Global Cancer Observatory: Cancer Today. Lyon: International Agency for Research on Cancer; 2020 [cited 2021 Jul 9]. Available from: https://gco.iarc.fr/today

[3] Alam T, Hu M, Isaacson RL. The role of growth hormone in metastasis and angiogenesis of breast cancer. Biosci Rep. 2026;46(2):BSR20253516.

[4] Szaefer H, Licznerska B, Sobierajska H, Baer-Dubowska W. Breast cancer cytochromes P450: chemopreventive and/or therapeutic targets for naturally occurring phytochemicals. Molecules. 2025;30(15):3079.

[5] Varela C, Amaral C, Gomes AR, Almeida CF, Correia-da-Silva G, Teixeira N, et al. Cutting-edge design approaches for steroidal aromatase inhibitors: new horizons for hormone-dependent cancer. Expert Opin Drug Discov. 2025;20(12):1655-81.

[6] Bilai IM, Dariy VI, Khilkovets AV, Bilai AI. Current research trends of 1,2,4-triazole derivatives biological activity (literature review). Curr Issues Pharm Med Sci Pract. 2025;18(2):197-205.

[7] Raman AP, Aslam M, Awasthi A, Ansari A, Jain P, Lal K, et al. An updated review on 1,2,3-/1,2,4-triazoles: synthesis and diverse range of biological potential. Mol Divers. 2025;29(1):899-964.

[8] Kedare SB, Singh RP. Genesis and development of DPPH method of antioxidant assay. J Food Sci Technol. 2011;48(4):412-22.

[9] Upadhyay N, Tilekar K, Oak A, Pokrovsky VS, Subramanian Chelakara R. Design, in silico studies, synthesis, and *in vitro* anticancer assessment of new naphthylidene isoxazolidinedione derivatives. Vietnam J Chem. 2024;62(2):217-26.

[10] Daharia A, Thakur AS, Dewangan L. A Computational Strategy for Validation of Piperidine as Lead from Phytochemical evaluation for Antiglycation activity via AGEs-RAGE Pathway Modulation. Journal of Pharma Insights and Research. 2025 Dec 5;3(6):273-84.

[11] Verma SK, Ratre P, Jain AK, Liang C, Gupta GD, Thareja S. De novo designing, assessment of target affinity and binding interactions against aromatase: discovery of novel leads as anti-breast cancer agents. Struct Chem. 2021;32(2):847-58.

[12] Kappe CO. Controlled microwave heating in modern organic synthesis. Angew Chem Int Ed Engl. 2004;43(46):6250-84.

[13] Shneine JK, Al-Majidi SM. Microwave assisted synthesis of some new 1,2,4-triazole derivatives as possible antimicrobial agents. Arab J Chem. 2016;9:S1201-7.